Surfactant-Free, Biodegradable Nanoparticles for Aerosol Therapy Based on the Branched Polyesters, DEAPA-PVAL-g-PLGA

L. A. Dailey,[1] E. Kleemann,[1,2] M. Wittmar,[1] T. Gessler,[2] T. Schmehl,[2] C. Roberts,[3] W. Seeger,[2] and T. Kissel[1,4]

Received June 18, 2003; accepted August 28, 2003

Purpose. This study describes the development of surfactant-free, biodegradable nanoparticle systems with varying physicochemical properties and their suitability for pulmonary application via nebulization.

Methods. Nanoparticle suspensions were formulated from the branched polyester, diethylaminopropyl amine-poly(vinyl alcohol)-grafted-poly(lactide-co-glycolide) (DEAPA-PVAL-g-PLGA) alone, as well as with increasing amounts of carboxymethyl cellulose (CMC). Particle size, ζ potential, turbidity, and morphology (atomic force microscopy) were characterized. Three formulations were chosen for further study: Cationic nanoparticles without CMC, cationic nanoparticles with CMC, and anionic nanoparticles with an excess of CMC. Nanoparticle degradation was characterized, as well as stability during nebulization. Nanoparticle-cell interactions were investigated and quantified using confocal laser scanning microscopy and fluorescence spectrometry.

Results. Nanoparticles ranged in size from 70–250 nm and displayed ζ potentials of +58.9 to −46.6 mV. Anionic nanoparticles showed the highest stability during nebulization. The degradation rate of each nanoparticle formulation decreased with increasing amounts of CMC. Cell association was highest among cationic nanoparticles (57% and 30%, respectively), although these were not internalized. Despite a lower rate of cell association (3%), anionic nanoparticles were internalized by A549 cells.

Conclusions. Surfactant-free nanoparticles from DEAPA-PVAL-g-PLGA are versatile drug delivery systems; however, only the anionic formulations investigated were proven suitable for aerosol therapy.

KEY WORDS: nanoparticles; aerosol; PLGA; lung; drug delivery.

INTRODUCTION

An enormous diversity of therapeutic agents is currently administered to patients via aerosol inhalation and the number of potential drug candidates for pulmonary application increases daily. The major areas of research are asthma (1), cysic fibrosis (2), lung cancer (3), tuberculosis (4,5), pulmonary hypertension (6), and diabetes (7,8). Issues complicating the development of aerosol formulations include compound loss during inhalation, dosing difficulties, enzymatic degradation within the lung, and the high costs of production. In several cases, the utilization of a controlled release system has the potential of overcoming many of these problems. Ideally, such a formulation must be able to be incorporated into an aerosol form, remain stable against forces generated during aerosolization, target a specific site or cell population in the lung, protect the compound against aggressive elements in the pulmonary tract, release the compound in a predetermined manner, be inert to the surrounding tissue, contain no irritating or toxic additives, and degrade when applicable within an acceptable period of time without producing toxic by-products (9,10).

Among the formulations currently being tested for pulmonary application, polymeric nanoparticles show promise in fulfilling the stringent requirements placed on these delivery systems. In the current study, nanoparticles have been formulated from a hydrophilic poly(lactide-co-glycolide) (PLGA) derivative, composed of short PLGA chains grafted onto an amine-substituted poly(vinyl alcohol) backbone (3-diethylamino-1-propylamine (8%)-poly(vinyl alcohol)-grafted-poly(lactide-co-glycolide)) (DEAPA-PVAL-g-PLGA) (Fig. 1). The amphiphilic properties of DEAPA-PVAL-g-PLGA make it highly suited for pulmonary formulations in several ways. Nanoparticles may be generated from DEAPA-PVAL-g-PLGA using a modified solvent displacement method without the use of customary surfactant stabilizers. This is of extreme importance for pulmonary application, as the inhalation of significant amounts of synthetic surfactants may disturb the naturally regulated surface tension of the pulmonary lining fluid, thus leading to impaired lung function or inflammation (11). Further, it has been discovered that the addition of varying amounts of a polyanion, such as carboxymethyl cellulose (CMC), dextran sulfate or even DNA, to the polymer during nanoparticle formulation can generate nanoparticles of variable physicochemical properties. This attribute can be used to design nanoparticle systems (e.g., cationic or anionic particles) for higher drug encapsulation efficiencies or greater stability in the face of shear forces.

Another aspect vital to the success of a polymeric drug delivery system in the lung is the rate of biodegradation, as well as the toxicity of degradation products. As many critics of pulmonary polymeric drug delivery have aptly pointed out, the prolonged degradation rates of most common biodegradable polymers, such as PLGA, are not suitable for application in the respiratory tract, especially when frequent administration is necessary. However, hydrophilic derivatization of PLGA, such as in the case of DEAPA-PVAL-g-PLGA, can have a dramatic effect on the rate of degradation by increasing the degree of water saturation within the particles and thereby enhancing hydrolytic degradation (12). Depending on the individual therapeutic regime of such a drug delivery system, a complete degradation of the particles within 1 week, or even 24 h, may be desired.

[1] Department of Pharmaceutics and Biopharmacy, Philipps University, Ketzerbach 63, 35037 Marburg, Germany.
[2] Department of Internal Medicine, Justus Liebig University, 35392 Giessen, Germany.
[3] Advanced Drug Delivery Group and Laboratory of Biophysics and Surface Analysis, School of Pharaceutical Science, University of Nottingham, Nottingham NG7 2RD, UK.
[4] To whom correspondence should be addressed. (e-mail: kissel@staff.uni-marburg.de)

ABBREVIATIONS: DEAPA-PVAL-g-PLGA, 3-diethylamino-1-propylamine (8%)-poly(vinyl alcohol)-grafted-poly(lactide-co-glycolide); CMC, carboxymethyl cellulose; RB, Rose Bengal; *0-CMC (+)*, Nanoparticle formulation containing 0 μg CMC / mg DEAPA-PVAL-g-PLGA; *5-CMC (+)*, Nanoparticle formulation containing 5 μg CMC / mg DEAPA-PVAL-g-PLGA; *50-CMC(−)*, Nanoparticle formulation containing 50 μg CMC / mg DEAPA-PVAL-g-PLGA

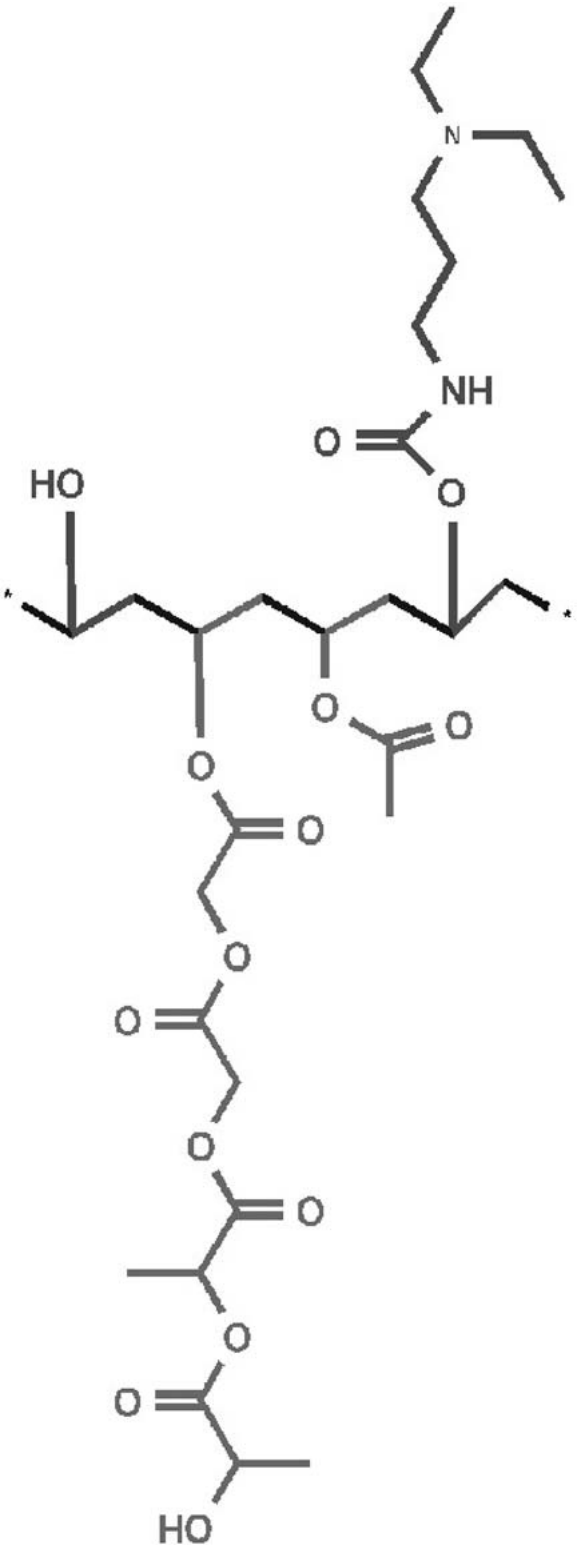

Fig. 1. DEAPA-PVAL-g-PLGA

MATERIALS AND METHODS

DEAPA-PVAL-g-PLGA was synthesized according to Wittmar *et al.* (13). Carboxymethyl cellulose (Tylopur® C 600) was purchased from Clariant (Sulzbach, Germany), 5-(4,6-dichlorotriazinyl) aminofluorescein (5-DTAF) from Molecular Probes (Leiden, The Netherlands), and Resomer® 503H was acquired from Boehringer Ingelheim (Ingelheim, Germany). All other chemicals were of analytical grade and purchased from Sigma Aldrich (Taufkirchen, Germany). Two different nebulizers were used in this study: the jet nebulizer, Pari® LC Star (Pari) (Pari Werk GmbH, Starnberg, Germany) and the ultrasonic nebulizer, Optineb® (Opti) (Nebutec, Elsenfeld, Germany). A549 cells were obtained from the German Collection of Microorganisms and Cell Cultures. Cells, passages 8–15, were maintained with DMEM supplemented with 10% fetal calf serum and 2 mM L-glutamine in an atmosphere of 8.5% CO_2 at 37°C and a relative humidity of 95%. A549 were seeded at a density of 1.0×10^4 cells / cm^2 and grown to confluency (approximately 72 h postseeding).

Preparation of Nanoparticle Suspensions

Nanoparticles were generated using a solvent displacement method, as described by Jung *et al.* (14) and modified in the following manner: 5 mg polymer, dissolved in 1.5 ml acetone, were slowly injected into 5 mL distilled water containing 0.01 M Tris-EDTA buffer pH 7.4 and, when applicable, varying amounts of CMC. The resulting suspensions were magnetically stirred for 3 h under reduced pressure to allow for removal of residual acetone.

Nanoparticle Characterization

The ζ-potential of the nanoparticles was measured in deionized water using a Malvern Zetasizer 3000 (Malvern Instruments GmbH, Herrenberg, Germany), while particle size was measured by photon correlation spectroscopy (PCS) at 90° through a 400 μm pinhole (Malvern Zetasizer 3000, Malvern Instruments GmbH, Herrenberg, Germany). The quality of each nanoparticle suspension could be estimated visually, as well as by turbidity measurements, using UV spectrometry (Ultraspec 1000, Pharmacia Biotech, Uppsala, Sweden) at a wavelength of 630 nm. Triplicate measurements of the % transmission of each sample were performed using distilled water as a reference.

Atomic Force Microscopy

Three nanoparticle formulations exhibiting varying physicochemical properties were chosen for further study. Formulation *0-CMC(+)* consisted of a nanoparticle suspension generated in the absence of any polyanion additive (cationic nanoparticles), formulation *5-CMC(+)* consisted of nanoparticles generated in the presence of 5 μg CMC/mg DEAPA-PVAL-g-PLGA (cationic nanoparticles), and formulation *50-CMC(–)* consisted of nanoparticles generated in the presence of 50 μg CMC/mg DEAPA-PVAL-g-PLGA (anionic nanoparticles). All imaging of the nanoparticles was performed using a Nanoscope IIIa multimode atomic force microscope (Veeco, Bicester, UK), operating in tapping mode in a liquid environment. A scan speed of approximately 2 Hz with 512 × 512 pixel resolution was used in all cases. Silicon nitride oxide-sharpened cantilevers were selected for this study, operating at resonant frequencies of approximately 10 kHz. A sample volume of 40 μl was spotted onto a 1 cm^2 disk of freshly cleaved mica. The addition of 10 mM nickel chloride

was necessary to initiate the attraction and immobilization of the negatively charged nanoparticles at the negatively charged mica surface. *0-CMC(+)* and *5-CMC(+)* were applied in undiluted form, whereas the anionic *50-CMC(−)* formulation, due to the excessively high concentration of nanoparticles, had to be diluted at a ratio of 1:10 in distilled water before application.

Nanoparticle Degradation

A method to characterize nanoparticle degradation was developed based upon a similar study by Shuai *et al.*, in which the accumulation of the polymer degradation products, lactic and glycolic acid, was quantified (15). Nanoparticle suspensions, *0-CMC(+)*, *5-CMC(+)*, and *50-CMC(+)* were prepared as described earlier. In addition, nanoparticles consisting of a commercially available poly (lactide-co-glycolide) polymer, Resomer® 503H (RG503H), were prepared in a 0.1% aqueous poloxamer solution (Pluronic® F68, Sigma Aldrich, Taufkirchen, Germany). The suspensions were incubated at 37°C while undergoing vertical rotation. 0.5 ml samples of each suspension were removed without volume replacement at predetermined time intervals. Nanoparticles or intact polymer molecules in the samples were precipitated with 0.5 mL 5% sodium chloride solution and centrifuged at ×4,000*g* for 30 min. The absorption intensity of the supernantant was measured at 205 nm in a UV spectrometer. The total amount of α-hydroxy acids in each sample was defined as the amount released after incubation of 5 mg polymer in 5 ml 0.1M potassium hydroxide solution for 4 weeks. Under these conditions, the PLGA chains were hydrolyzed to lactic/glycolic acid and detected at 205 nm. Calibration curves from each hydrolyzed polymer sample were used to calculate the percent of released α-hydroxy acids and negative controls of all formulations without the addition of polymer were used to set baseline absorption.

Stability During Nebulization

The stability of the nanoparticle suspensions during aerosolization was qualitatively investigated using Fraunhofer laser diffraction (Sympatec GmbH, Clausthal–Zellerfeld, Germany). Briefly, samples of 5 ml suspension (*5-CMC(+)* and *50 CMC(−)*) were nebulized with the Pari® LC Star and the Optineb®. Nebulization was carried out at an airflow rate of 10 L/min for a total of 10 min. Samples of the nebulized aerosol were collected by placing a glass microscopic slide in front of the nebulizer mouthpiece and allowing the aerosol droplets to deposit on the glass. The resulting condensation fluid was collected in Eppendorf tubes for further analysis. Aliquots of the non-nebulized nanoparticle suspensions and the suspensions after nebulization were added to a cuvette filled with 29 mL distilled water and measured via laser diffractometry.

Labeling of DEAPA-PVAL-g-PLGA With 5-DTAF

Ten milligrams DEAPA-PVAL-g-PLGA were dissolved in 400 μl acetone and slowly injected into 2 ml 0.03 Tris-EDTA buffer pH 9.0. The mixture was stirred magnetically for 2 h to remove residual acetone. 260 μg 5-DTAF (dissolved in 26 μl dimethyl sulfoxide) were added to the mixture and allowed to react under light exclusion for 1.5 h at 60–70°C. Free 5-DTAF was separated from bound 5-DTAF via size exclusion chromatography using a Sephadex G-25 column (PD10, Pharmacia, Freiburg, Germany) with a 10 kD cut-off. The aliquot of labeled polymer (~2 ml) was lyophilized for a minimum of 48 h (Christ β-01, Christ, Osterode, Germany). A recovery of 30–50% labeled polymer was generally achieved.

Quantitative Determination of Nanoparticle-Cell Interactions

Cell association was determined by incubating A549 cells seeded on 24 well polystyrene dishes (growth area: 1.9 cm^2) (Nunc, Wiesbaden, Germany) with the nanoparticle suspensions and subsequent quantitation was performed via fluorescence spectrometry (LS 50 B, Perkin–Elmer, Rodgau–Jügesheim, Germany). Fluorescent-labeled nanoparticles were prepared as previously described using a polymer mixture of 90% DEAPA-PVAL-g-PLGA and 10% 5-DTAF-DEAPA-PVAL-g-PLGA. A subset of double-labeled nanoparticle suspensions was also prepared by encapsulating 8.95 mol Rose Bengal (RB)/mol DTAF-DEAPA-PVAL-g-PLGA (2% theoretical loading) in the nanoparticles. An encapsulation efficiency of approximately 97% was achieved. All nanoparticle suspensions were diluted with an equivalent volume of 10% glucose solution to achieve isotonicity. Cells were incubated with 0.5 ml of each nanoparticle suspension for 60 min. at 37°C, 8.5% CO_2, and 95% r.h. Following incubation, the suspension was removed and the cells were washed three times with ice-cold 5% glucose. The cell layers were allowed to dry at room temperature under light exclusion and were subsequently lysed in 200 μl 50 mM EDTA / 2% Triton-X pH 8.0. The amount of cell-associated fluorescence was quantified at the following wavelengths: 5-DTAF excitation = 488 nm, 5-DTAF emission = 525 nm, RB excitation = 540 nm, and RB emission = 567 nm.

Confocal Laser Scanning Microscopy

Cells grown on glass chamber slides (Lab-Tek® II, growth area: 4.0 cm^2, Nunc, Wiesbaden, Germany) were incubated for 60 min with 1 ml isotonic nanoparticle suspension and washed as previously described. The cell layers were subsequently fixed with 3% (v/v) formalin in phosphate buffered saline solution and counterstained with TRITC-labeled maclura pomifera agglutinin (MPA, 0.01μg/ml) and 4′6-diamidino-2-phenylindole (DAPI, 1μg/ml) for 20 min under light exclusion. The cells were embedded in FluorSave® (Merck Biosciences, Darmstadt, Germany) and examined under a confocal laser scanning microscope (Axiovert™, Zeiss CLSM 501, Jena, Germany) equipped with a Zeiss Neofluor 100*/1.3 oil immersion objective. Excitation wavelengths were 364 nm (long pass filter (LP) 385 nm) for DAPI, 488 nm (LP 505 nm) for 5-DTAF, and 543 nm (LP 560 nm) for TRITC and RB. A gallery of 40 optical slices (0.4 μm) was collected and xz, yz composites were processed using Zeiss LSM 510™ software. Sensitivity was kept constant during different experiments.

Statistical Analysis

Statistical calculations were carried out with SPSS 9.0 for Windows (SPSS GmbH, Munich, Germany). All values were presented as the mean ± standard deviation unless otherwise

noted. Statistical comparisons were performed using nanoparticle aired Student's *t* tests after prior evaluation of normal distribution via Kolmogorov–Smirnov tests. In the case of multiple testing, the Holm correction was applied (16). Probability values $p < 0.05$ were considered significant.

RESULTS

Nanoparticle Characterization

Eight nanoparticle formulations were generated with increasing amounts of CMC and were characterized with regard to particle size, ζ-potential, and turbidity (Table I). Nanoparticle formation was highly dependent upon the ζ-potential of the nascent nanoparticles. Only particles displaying a pronounced positive or negative charge were able to form stable nanoparticle suspensions, whereas formulations exhibiting a ζ-potential close to neutrality, approximately 10–50 μg CMC / mg DEAPA-PVAL-g-PLGA, showed immediate polymer agglomeration. Nanoparticle size measurements and turbidity studies also mirrored this trend. Nanoparticle diameters, as well as the visual cloudiness of the suspensions, grew with increasing neutrality. While formulations without CMC showed nearly 100% transmission, nanoparticles containing CMC were generally opalescent with a higher transmission among the positively charged suspensions. Anionic nanoparticle suspensions displayed a definite opalescence and transmission rates ranging from 60–70%.

Three representative nanoparticle formulations were visualized using AFM (see Fig. 2). It was shown that *0-CMC(+)* consisted exclusively of free DEAPA-PVAL-g-PLGA, which had formed tiny spheres of approximately 20–40 nm (see Fig. 2A). *5-CMC(+)* contained larger nanoparticles (100–200 nm) interspersed amid a background of free DEAPA-PVAL-g-PLGA (see Fig. 2B), while absolutely no free DEAPA-PVAL-g-PLGA was detectable within the *50-CMC(−)* formulation (see Fig. 2C). This was verified by images taken from samples of *50-CMC(−)* on mica without nickel chloride pretreatment. In this case, no cationic polymer or nanoparticle structure could be observed attached to the negatively charged mica (data not shown). In contrast, pretreatment with nickel chloride resulted in images displaying a large, homogenous population of nanoparticles ranging in size from 150–250 nm.

Table I. Eight Nanoparticle Formulations Were Generated with Increasing Amounts of CMC and Were Subsequently Characterized with Regard to Particle Size (PCS), ζ-Potential (Laser Doppler Anenometry) and Turbidity (UV Spectrometry)

CMC concentration (μg CMC/ mg polymer)	Particle size (nm)	Zeta potential (mV)	Turbidity (% transmission)
0	76.2 ± 8.8	58.9 ± 1.9	96.4
5	177.8 ± 1.0	47.6 ± 1.7	88.9
10*	241.4 ± 1.9*	45.7 ± 0.7*	88.7*
20**	256.6 ± 4.6**	39.9 ± **	86.0**
50	202.5 ± 2.9	−16.6 ± 0.3	63.6
100	202.5 ± 1.5	−23.0 ± 0.5	72.4
200	215.5 ± 2.9	−28.4 ± 0.4	62.2
400	213.6 ± 3.0	−46.6 ± 1.1	71.4

The asterisks denote cases in which polymer precipitation and flocculation occurred (* light flocculation, ** heavy flocculation).

Nanoparticle Degradation

Degradation profiles based on mass loss and molecular weight determinations have been performed with polymers of this class and have shown rapid degradation within 2–7 days (17). These methods, however, do not take into account nanoparticle size and morphology, as well as other formulation components, such as CMC or potential drug compounds, which may influence the degradation rate. A suitable method to characterize polymer degradation from nanoparticles has not yet been devised and the method used in this study can only provide information on the release rate of degradation products. Despite this, valuable information regarding the influence of formulation parameters on α-hydroxy acid release could be obtained.

A consequence of the stabilizing effect of CMC on nanoparticle formulations was a significant decrease in the rate of degradation between nanoparticle formulations with and without CMC (Fig. 3). Although *0-CMC(+)* had released 86.9 ± 2.2% α-hydroxy acids after 4 weeks incubation, *5-CMC(+)* had released 80.6 ± 2.6% and *50-CMC(−)* only 65.3 ± 4.7%. The slower degradation rate of the *50-CMC(−)* formulation, most likely due to the increase in hydrophobicity caused by a neutralization of the polymer charge, is, in comparison to the degradation rate of RG 503H (only 25.2 ± 3.1% after 4 weeks), a significant acceleration. The burst effect seen in the initial 24 h results, in part, from the presence of free lactic and glycolic acid residues within the polymer, which were detected via gas chromatography.

Stability During Nebulization

Figure 4 depicts a typical volume distribution curve measured by Fraunhofer laser diffraction before and after nebulization of the nanoparticle suspensions with both the Pari® LC Star and Optineb®. As previously discussed in (18), limitations of the Fraunhofer theory restrict the applicability of this method for the exact determination of particle sizes <500 nm. Despite this, laser diffractometry has proven an excellent means of determining changes in particle size populations before and after nebulization. As Figs. 4A–D demonstrate, both *5-CMC(+)* and *50-CMC(−)* nanoparticle populations were small and uniformly distributed before nebulization. In contrast, laser diffraction analysis of the collected nebulized suspension *5-CMC(+),* as well as from the residual reservoir fluid (data not shown) of both nebulizers, showed a bimodal size distribution pattern implying that particle aggregation indeed took place during the nebulization process (see Fig. 4A,C). This was verified by AFM images taken from the nebulized samples (see Fig. 4E,G). Furthermore, visible polymer aggregation was observed in the reservoir compartments of both nebulizers. Nebulization of *50-CMC(−)*, on the other hand, had absolutely no effect on the nanoparticle size distribution regardless of nebulizer type (see Fig. 4B,D), as also verified by AFM images (see Fig. 4F,H). Due to the extremely small size of the polymer structures in *0-CMC(+)* (20–40 nm), it was not possible to characterize this formulation using laser diffractometry. However, nebulization of *0-CMC(+)* also led to visible polymer aggregation in both nebulizer reservoirs. This observation implied that free DEAPA-PVAL-g-PLGA was unstable during jet and ultrasonic nebulization, while nanoparticles created from this

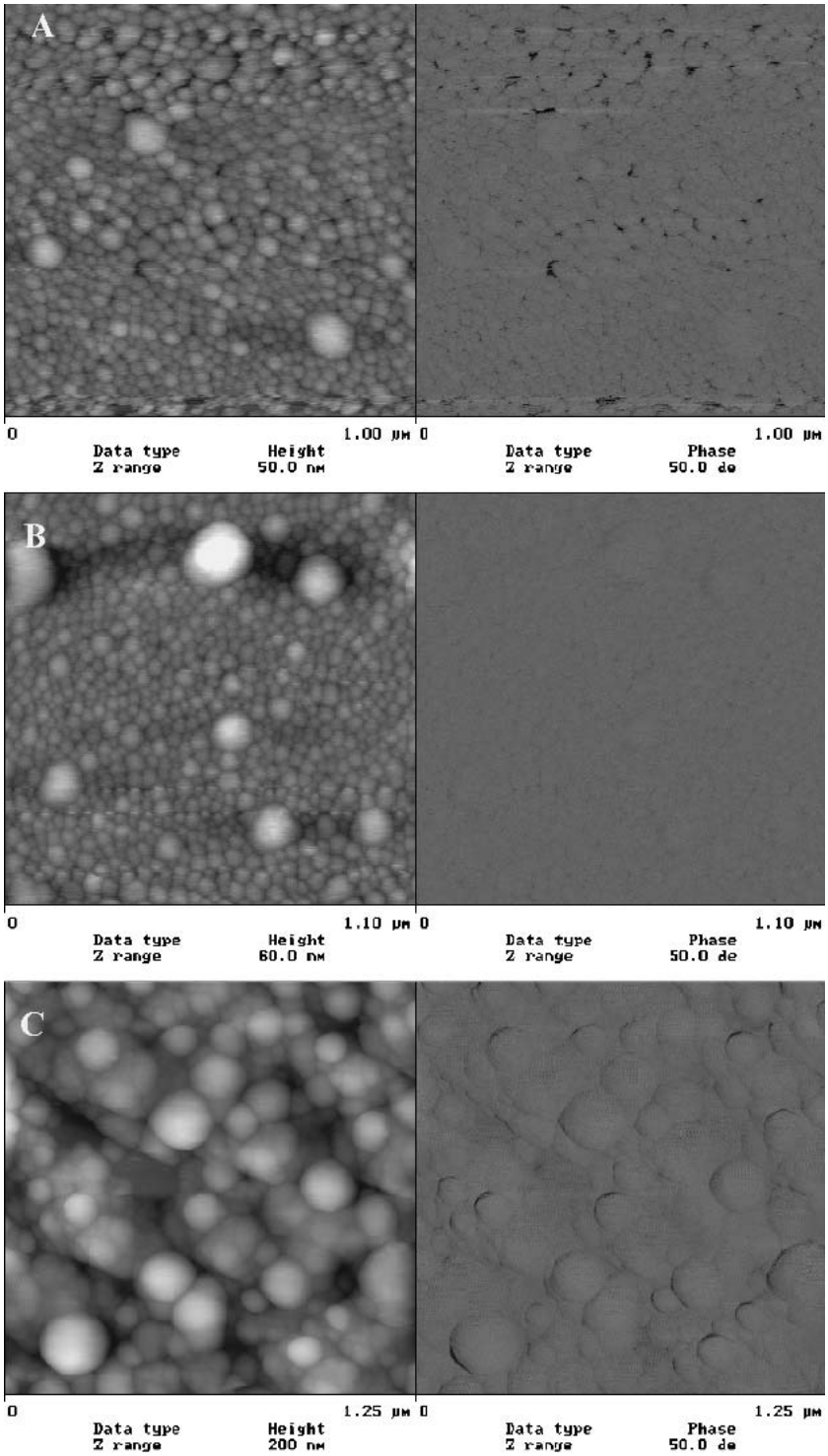

Fig. 2. AFM images of three representative nanoparticle formulations. A) *0-CMC(+),* B) *5-CMC(+)*, C) *50-CMC(–)*.

polymer showed absolutely no tendency toward aggregation. This theory also provides an explanation for the partial instability of *5-CMC(+)* during nebulization, as this formulation contained significant amounts of free DEAPA-PVAL-g-PLGA.

Nanoparticle-Cell Interactions

Figure 5 shows CLSM images taken after cells had been incubated with all three formulations for 60 min. It could be clearly shown that the surface charge of the particles had a dramatic effect on cell interactions. The cationic formulations exhibited an extremely high affinity for the cell membrane (see Fig. 5A–C). Internalization of the free polymer or particles, by means such as adsorptive endocytosis, apparently did not occur within the investigated time period. Nanoparticles from the anionic formulation, *50-CMC(–)*, did not demonstrate an affinity toward the cell membrane (see Fig. 5D,E). However, CLSM images showed that *50-CMC(–)* nanopar-

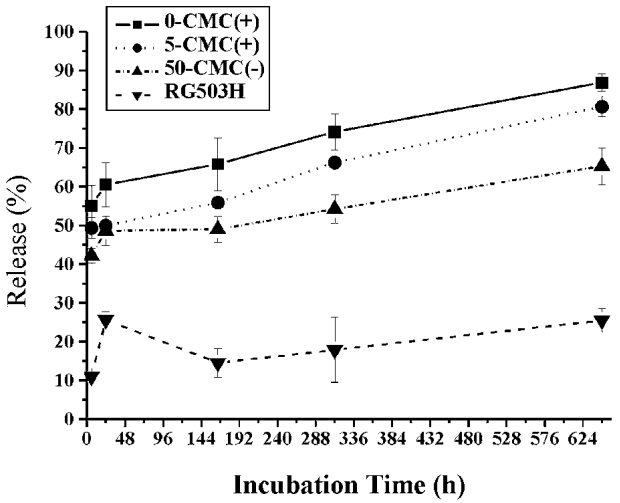

Fig. 3. Release of lactic / glycolic acid from nanoparticle suspensions as a measure of nanoparticle degradation over a time period of four weeks (n = 3). The amount of degradation products released from *5-CMC(+)*, *50-CMC(–)*, and RG503H after four weeks incubation differed significantly from that of the free polymer, *0-CMC(+)* ($p > 0.05$).

ticles were internalized to some extent (see Fig. 5E), although the mechanism remains unclear.

Cell association of the different formulations was quantified using fluorescence spectrometry (Fig. 6). As seen in the CLSM images, *0-CMC(+)* displayed the highest degree of cell association (57.6 ± 2.8%). *5-CMC(+)* exhibited a 2-fold decrease in cell association (30.6 ± 5.6%), whereas only 2.9 ± 0.7% of the *50-CMC(–)* nanoparticles were actually taken up by the cells. The amount of the encapsulated model drug, RB, did not significantly differ from the detected amount of 5-DTAF, implying that RB remained incorporated within the nanoparticles for the duration of the study. This was also confirmed by the confocal images of nanoparticles containing RB, in which the colocalization of the two fluorophores is easily seen (see Fig. 5B, F). The anionic nature of RB influenced the formation of nanoparticles in the same manner, although to a weaker extent, as CMC. This resulted in polymer agglomeration of *5-CMC(+)* containing RB and, therefore, quantification of cell association, as well as CLSM studies, could not be performed with this formulation.

DISCUSSION

The most highly publicized breakthrough in the pulmonary delivery of controlled release systems was made in 1997 with the development of large, porous particles (LPP) for dry powder inhalation (19). These PLGA microparticles showed enhanced aerodynamic properties enabling such large particles to be delivered to the peripheral regions of the lung and were proposed to avoid macrophage clearance by virtue of size alone. However, a disadvantage of the original LPP was the slow rate of PLGA degradation in the lung periphery, resulting from the large size of the particles and small area of fluid contact.

This problem has since been addressed by several groups. The major trend is to move away from PLGA as the biodegradable polymer of choice for pulmonary delivery systems and instead concentrate on synthesizing polymers that degrade within a much shorter timespan. Fu *et al.*, for example, have developed ether-anhydride copolymers, composed of sebacic acid and copolymerized with PEG, for pulmonary microparticle delivery (20). For several years, our lab has been synthesizing biodegradable branched polyesters consisting of PLGA chains grafted to a PVAL backbone for use in a wide spectrum of drug delivery systems. Due to the hydrophilic PVAL backbone, these polymers were especially useful for the encapsulation of highly sensitive molecules, such as proteins or peptides (15,21–23). Further derivatization of this polymer class has led to a new generation of charge-modified branched polyesters to which DEAPA-PVAL-g-PLGA belongs. These new polymers have proven extremely useful by utilizing electrostatic interactions to further increase encapsulation efficiencies of drug molecules. Another positive aspect is the fact that by varying the degree of amine substitution or PLGA side-chain to backbone ratio, a spectrum of polymers could be synthesized displaying almost any chosen rate of degradation.

Although most studies of pulmonary drug delivery systems have used microparticles to deliver their contents via dry powder inhalation to the respiratory tract (24), few have shown interest in nanoparticle systems. Realizing the advantages of nanoparticle technology, Tsapis *et al.* optimized the LPP by developing "trojan particles" for pulmonary drug delivery (25), which are essentially LPP comprised of spray-dried nanoparticle suspensions. They claim to combine the positive aerodynamic aspects of LPP with the attractive drug delivery properties of nanoparticles. Although achieving this to an extent, the main disadvantage of the trojan particles is the dependence on non-biodegradable polystyrene or silica nanoparticles for LPP formulation. The application of non-biodegradable systems in the lung is questionable, especially in cases where multiple dosing is required.

In comparison to other systems, the anionic nanoparticle formulations described in this study avoid many such obstacles. For example, alveolar deposition can be easily achieved by either jet or ultrasonic nebulization of the nanoparticle suspensions, regardless of the aerodynamic properties of the nanoparticles themselves. One important observation made in this study was the influence of the formulation on stability during nebulization. Our previous studies demonstrated clearly that a certain degree of polymer hydrophilicity was essential to prevent particle aggregation within aerosolized fluid droplets during nebulization. Especially high aggregation rates were observed, for example, among hydrophobic PLGA particles during jet nebulization (18). In the present study, it was further demonstrated that not only polymer hydrophilicity was necessary for stability during nebulization, but also the formation of well-defined nanoparticles. Formulations containing free DEAPA-PVAL-g-PLGA showed high amounts of aggregated polymer and, therefore, only anionic formulations could be nebulized efficiently. In contrast to our previous study, in which most hydrophilic nanoparticles showed a small percent of aggregation (18), nebulization did not have any effect on the *50-CMC(–)* nanoparticles.

The acquisition of highly defined nanoparticles from DEAPA-PVAL-g-PLGA was shown to be dependent on nanoparticle formulation. Based on the physico-chemical data, it was postulated that DEAPA-PVAL-g-PLGA formed a colloidal, highly cationic polymer suspension in water when

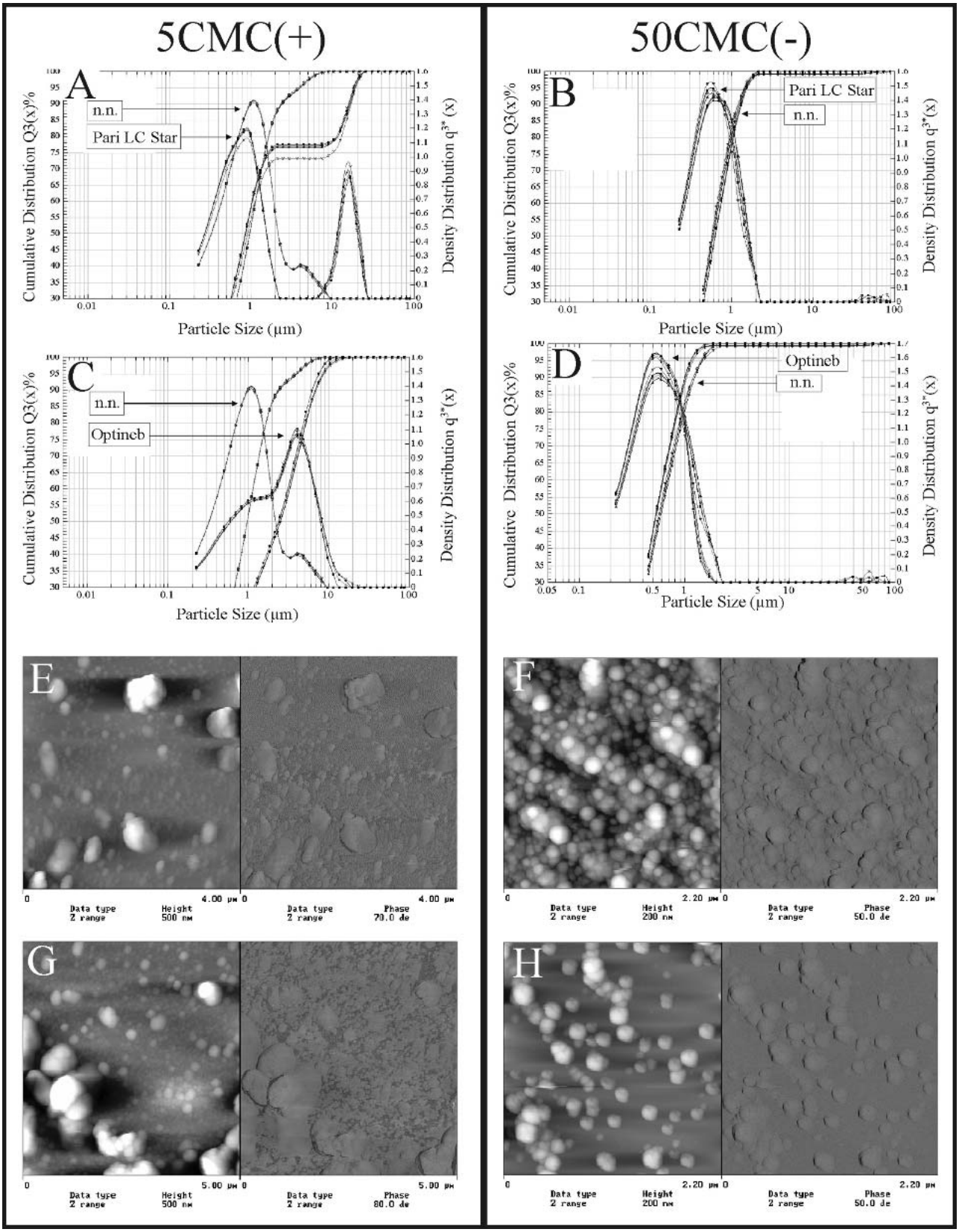

Fig. 4. Stability of the nanoparticle suspensions, *5-CMC(+)* and *50-CMC(–)*, during jet and ultrasonic nebulization. Figures 4A–D show the size distributions of nanoparticle suspensions before and after nebulization as measured by Fraunhofer laser diffractometry. Figures 4E–H show the corresponding AFM images of nebulized nanoparticle suspensions. 4E) *5-CMC(+)* after nebulization with the Pari® LC Star, 4F) *50-CMC(–)* after nebulization with the Pari® LC Star, 3G) *5-CMC(+)* after nebulization with the Optineb®, 3H) *50-CMC(–)* after nebulization with the Optineb®.

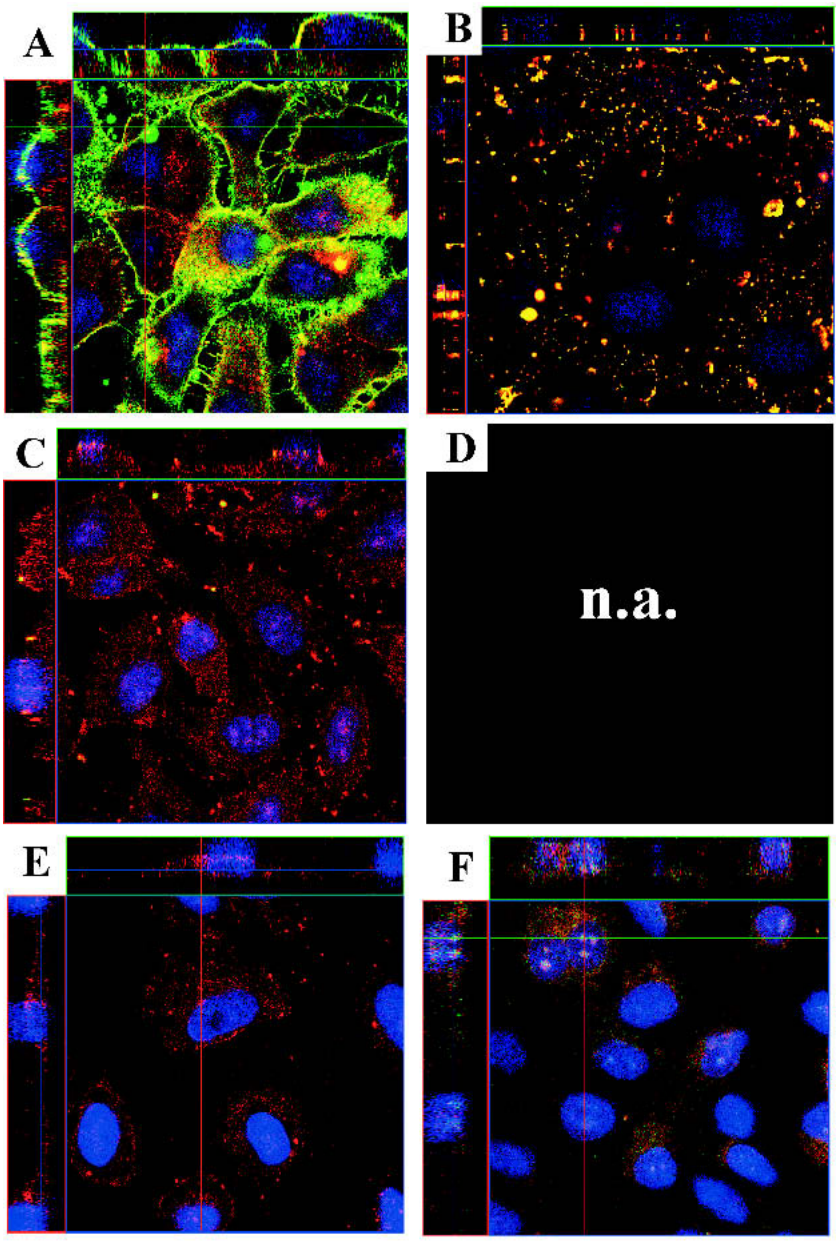

Fig. 5. Cell association after 60 min incubation with three nanoparticle suspensions. 5A) *0-CMC(+)*, 5B) *0-CMC(+)* + RB, 5C) *5-CMC(+)*, 5D) images not available, 5E) *50-CMC(−),* 5F) *50-CMC(−)* + RB.

applied in the absence of an opposite charge (*0-CMC(+)*), whereas the addition of increasing amounts of CMC to the aqueous phase resulted in the precipitation of nanoparticles within the colloidal polymer suspension. It may be assumed that the net charge of the polymer was neutralized during the complexation process with CMC, which ultimately led to a higher degree of lipophilicity and precipitation to nanoparticles. It is likely that a small percent of the free polymer was absorbed onto the particle surface causing an electrostatic repulsion among the particles, explaining the higher stability in suspension (*5-CMC(+)*). A further increase in the amount of CMC (10–50 μg/mg polymer) very likely left the nanoparticles insufficiently coated with free cationic DEAPA-PVAL-g-PLGA and thus prone to agglomeration. Only after a critical CMC concentration had been exceeded (≥50 μg CMC/mg polymer) were free CMC molecules able to sufficiently coat all precipitated nanoparticles and prevent agglomeration (*50-CMC(−)*).

Another major advantage of DEAPA-PVAL-g-PLGA nanoparticles over those made from PLGA is the surfactant-free formulation. Although in many cases synthetic surfactants may be acceptable excipients for oral or even intravenous application, these agents may significantly disturb lung function and also disrupt the nebulization process of most nebulizers as a result of intense foaming. The only additive needed to generate DEAPA-PVAL-g-PLGA nanoparticles is a negatively charged anion (ideally a polyanion), which is required for complexation with the cationic amino moieties of the PVAL chain. In this study, CMC, a common pharmaceutical excipient, was chosen as a stabilizer; however, the role of

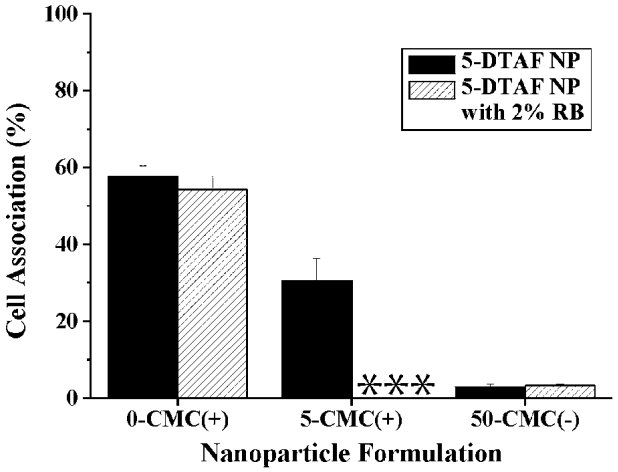

Fig. 6. Quantitative analysis of cell association via fluorescence spectroscopy (n = 3). A comparison of the respective amounts of 5-DTAF and RB associated with the cells showed no statistically significant difference, implying that the model compound, RB, remained incorporated within the nanoparticles for the duration of the experiment ($p > 0.05$). *** Quantitative analysis could not be performed.

CMC may be substituted by any other polyanion, including dextran sulfate, which has been previously used in the pulmonary tract as a mucolytical agent in cystic fibrosis research (26), or even DNA for use in gene therapy (13).

Most properties of the anionic nanoparticle systems investigated in this study make this formulation the most suitable for pulmonary drug delivery. However, a major disadvantage of the *50-CMC(–)*nanoparticles was their extremely low rate of *in vitro* cell association. Electrostatic repulsion between the anionic nanoparticles and the negatively charged cell membrane lowered the probability of nanoparticle-cell interactions dramatically. However, it was surprising to observe that, while cell association was low, actual particle internalization could be detected in the CLSM images. The cationic formulations, *0-CMC(+)* and *5-CMC(+)*, displayed the opposite effect. In this case, electrostatic interactions with the membrane components were responsible for the high affinity to the membrane of the A549 cells, albeit without any evidence of internalization.

Although *in vitro* studies may provide clues to the behavior of such systems *in vivo*, they cannot replace *in vivo* models. Because of this fact, further studies with optimized nanoparticle systems, such as *50-CMC(–)*, in *in vivo* models are essential for complete characterization. Future questions of interest include nanoparticle deposition patterns in the lung after aerosol application, residence time of the nanoparticles in the lung, and toxicology or biocompatibility studies. Of particular interest may also be the question as to whether biodegradable nanoparticles trigger the same inflammatory response in the lung as "ultrafine particles" of other materials have been shown to do (27). Finally, once the safety of these nanoparticle systems has been established, their efficacy as drug carriers using relevant therapeutic compounds remains to be characterized.

REFERENCES

1. A. Pahl and I. Szelenyi. Asthma therapy in the new millennium. *Inflamm. Res.* **51**:273–282 (2002).
2. L. Garcia-Contreras and A. J. Hickey. Pharmaceutical and biotechnological aerosols for cystic fibrosis in therapy. *Advan. Drug Delivery Rev.* **54**:1491–1504 (2002).
3. S. Sharma, D. White, A. R. Imondi, M. E. Placke, D. M. Vail, and M. G. Kris. Development of inhalational agents for oncological use. *J. Clin. Oncol.* **19**:1839–1847 (2001).
4. S. Suarez, P. O'Hara, M. Kazantseva, C. E. Newcomer, R. Hopfer, D. N. McMurray, and A. J. Hickey. Airways delivery of rifampicin microparticles for the treatment of tuberculosis. *J. Antimicrob. Chemother.* **48**:431–434 (2001).
5. R. Sharma, D. Saxena, A. K. Dwivedi, and A. Misra. Inhalable microparticles containing drug combinations to target alveolar macrophages for treatment of pulmonary tuberculosis. *Pharm. Res.* **18**:1405–1410 (2001).
6. B. Zwissler. Inhaled vasodilators. *Anaesthesist.* **51**:603–624 (2002).
7. D. R. Owens. New horizons—Alternative routes for insulin therapy. *Nat. Rev. Drug Discov.* **1**:529–540 (2002).
8. J. S. Patton, J. Bukar, and S. Nagarajan. Inhaled insulin. *Advan. Drug Delivery Rev.* **35**:235–247 (1999).
9. D. A. Edwards and C. Dunbar. Bioengineering of therapeutic aerosols. *Annu. Rev. Biomed. Eng.* **4**:93–107 (2002).
10. R. W. Niven. Delivery of biotherapeutics by inhalation aerosol. *Crit. Rev. Ther. Drug Carr. Syst.* **12**:151–231 (1995).
11. M. Suzuki, M. Machida, K. Adachi, K. Otabe, T. Sugimoto, M. Hayashi, and S. Awazu. Histopathological study of the effects of a single intratracheal instillation of surface active agents on lung in rats. *J. Toxicol. Sci.* **25**:49–55 (2000).
12. A. Breitenbach, K. F. Pistel, and T. Kissel. Biodegradable comb polyesters. Part II. Erosion and release properties of poly(vinyl alcohol)-g-poly(lactic-*co*-glycolic acid). *Polymer* **41**:4781–4792 (2000).
13. M. Wittmar and T. Kissel. The synthesis of polyesters with amine-modified poly(vinyl alcohol) backbones: A novel class of positively charged biopolymers for drug delivery and DNA vaccination. *Europolymer Congress,* Eindhoven (2001).
14. T. Jung, A. Breitenbach, and T. Kissel. Sulfobutylated poly(vinyl alcohol)-graft-poly(lactide-co-glycolides) facilitate the preparation of small negatively charged biodegradable nanospheres. *J. Cont. Rel.* **67**:157–169 (2000).
15. X. Shuai, M. Wei, F. E. Porbeni, T. A. Bullions, and A. E. Tonelli. Formation of and Coalescence from the Inclusion Complex of a Biodegradable Block Copolymer and α-Cyclodextrin. 2: A Novel Way to Regulate the Biodegradation Behavior of Biodegradable Block Copolymers. *Biomacromolecules* **3**:201–207 (2002).
16. S. Holm. A simple sequentially rejective multiple test procedure. *Scand. J. Statistics* **6**:65–70 (1979).
17. F. Unger, M. Wittmar, and T. Kissel. Branched polyesters of the type PVAL-g-PLGA allow design of rapidly degrading parenteral delivery systems. *Proceedings 30th International Symposium on rolled Release of Bioactive Materials*, Glasgow, Scotland 499 (2003).
18. L. A. Dailey, T. Schmehl, T. Gessler, M. Wittmar, F. Grimminger, W. Seeger, and T. Kissel. Nebulization of biodegradable nanoparticles: Impact of nebulizer technology and nanoparticle characteristics on aerosol features. *J Cont. Rel.* **86**:131–144 (2003).
19. D. A. Edwards, J. Hanes, G. Caponetti, J. Hrkach, A. Ben–Jebria, M. L. Eskew, J. Mintzes, D. Deaver, N. Lotan, and R. Langer. Large Porous Particles for Pulmonary Drug Delivery. *Science* **276**:1868–1871 (1997).
20. J. Fu, J. Fiegel, E. Krauland, and J. Hanes. New polymeric carriers for controlled drug delivery following inhalation or injection. *Biomaterials* **23**:4425–4433 (2002).
21. A. Breitenbach and T. Kissel. Biodegradable comb polyesters: Part 1—Synthesis, characterization and structural analysis of poly(lactide) and poly(lactide-co-glycolide) grafted onto water-soluble poly(vinyl alcohol) as backbone. *Polymer* **39**:3261–3271 (1998).
22. K. F. Pistel, A. Breitenbach, R. Zange–Volland, and T. Kissel. Brush-like branched biodegradable polyesters, part III—Protein release from microspheres of poly(vinyl alcohol)-graft-poly(D,L-lactic-co-glycolic acid). *J. Cont. Rel.* **73**:7–20 (2001).

23. T. Jung, W. Kamm, A. Breitenbach, G. Klebe, and T. Kissel. Loading of tetanus toxoid to biodegradable nanoparticles from branched poly(sulfobutyl-polyvinyl alcohol)-g-(lactide-co-glycolide) nanoparticles by protein adsorption: a mechanistic study. *Pharm. Res.* **19**:1105–1113 (2002).
24. H. M. Courrier, N. Butz, and T. F. Vandamme. Pulmonary drug delivery systems: recent developments and prospects. *Crit. Rev. Ther. Drug Carrier Syst.* **19**:425–498 (2002).
25. N. Tsapis, D. Bennett, B. Jackson, D. A. Weitz, and D. A. Edwards. Trojan particles: Large porous carriers of nanoparticles for drug delivery. *Proc. Natl. Acad. Sci. USA* **99**:12001–12005 (2002).
26. E. Sudo, W. A. Boyd, and M. King. Effects of dextran sulfate on tracheal mucociliary velocity in dogs. *J. Aerosol Med.* **13**:87–96 (2000).
27. D. M. Brown, M. R. Wilson, W. MacNee, V. Stone, and K. Donaldson. Size-dependent proinflammatory effects of ultrafine polystyrene particles: a role for surface area and oxidative stress in the enhanced activity of ultrafines. *Toxicol. Appl. Pharmacol.* **175**: 191–199 (2001).